



Published in final edited form as:

Chemistry. 2010 December 3; 16(45): 13325–13329. doi:10.1002/chem.201002360.

## Synthesis of Macrocyclic Tetrazoles for Rapid Photoinduced Bioorthogonal 1,3-Dipolar Cycloaddition Reactions

Dr. Zhipeng Yu, Reyna K. V. Lim, and Prof. Dr. Qing Lin\*

Department of Chemistry, State University of New York at Buffalo, Buffalo, NY 14260, USA, Fax: (+01) 716-645-6963

### Abstract

A series of conformationally constrained, macrocyclic tetrazoles were expediently prepared by double alkylation of a bis(*o*-phenyl)tetrazole precursor. Several of them showed excellent reactivity toward norbornene in a photoinduced tetrazole-alkene cycloaddition reaction in organic solvent as well as toward a norbornene-modified protein in PBS buffer.

### Keywords

bioorthogonal chemistry; tetrazole; alkene; cycloaddition; biotechnology

There is increasing interest to develop robust bioorthogonal reactions for site-specific modification of biomolecules within living systems.[1] A prominent example is the copper-catalyzed azide-alkyne cycloaddition reaction (“CuAAC”).[2] Since copper is toxic to cells, there have been substantial efforts directed toward developing copper-free alternatives for applications in live cells. One strategy involves activation of dipolarophiles by constraining them in macrocyclic rings: several cyclooctynes have been developed for rapid 1,3-dipolar cycloadditions with azide.[3] However, the use of ring structures containing strained dipoles for rapid bioorthogonal 1,3-dipolar cycloaddition reactions was extremely rare,[4] despite the fact that many cyclic dipoles have been used successfully in organic synthesis, e.g., cyclic azomethine imine,[5] cyclic carbonyl ylide,[6] cyclic azomethine ylide,[7] and cyclic nitrones[8] (Scheme 1). To our knowledge, cyclic nitrile imines—an important class of 1,3-dipoles[9] for the preparation of pyrazolines—has not been reported in the literature.

We have recently reported the use of diaryltetrazoles as photoactivatable precursors to the reactive nitrile imine dipoles for a photoinduced, bioorthogonal cycloaddition reaction with both the electron-deficient alkenes[10] and the unactivated terminal alkenes.[11] In a photocrystallographic study, we found that upon photoirradiation a diaryltetrazole generated *in situ* a bent nitrile imine,[12] the geometry postulated to exhibit reduced distortion energy and thus higher reactivity based on recent computational studies.[13] To reinforce the nitrile imine geometry in this reactive conformation, we hypothesized that installing a short “bridge” between the *ortho*-positions of two flanking phenyl rings to form a macrocyclic diphenyltetrazole should generate a cyclic nitrile imine upon photoirradiation with an overall reduced rotational freedom. Toward this goal, here we report the synthesis of a series of conformationally constrained macrocyclic tetrazoles and the characterization of their reactivity toward both a terminal alkene and a strained alkene in organic solvents as well as a norbornene-modified lysozyme in phosphate buffered saline (PBS).

qinglin@buffalo.edu.

Supporting information for this article is available on the WWW under <http://www.chemeurj.org/> or from the author.

To create the attachment sites for the installation of a chemical “bridge”, we synthesized two linear tetrazoles, 2,5-bis(*o*-phenolyl)-tetrazole (**1**) and 2-*o*-phenolyl-5-*o*-anilinyltetrazole (**7**) using the Kakehi method.[14] To effect macrocyclization via bis-alkylation, we treated tetrazole **1** with 1.1 equiv of dibromoalkanes with variable carbon length and screened four alkali metal bases: LiOH, Na<sub>2</sub>CO<sub>3</sub>, K<sub>2</sub>CO<sub>3</sub> and Cs<sub>2</sub>CO<sub>3</sub>, anticipating that alkali metal ions with the right size may facilitate ring closure by bringing two phenol-O to the N1-side of tetrazole **1** through chelation (Table 1). Gratifyingly, we found that bases with larger alkali metals such as Cs<sup>+</sup> and K<sup>+</sup> in general afforded higher yields of the desired macrocyclic products (entries 7–8, 11–12, 15–16, and 19–20). Yields were lowest for tetrazole **2** (entries 3–4), presumably due to its smallest ring size (12-membered ring). Li<sup>+</sup> and Na<sup>+</sup> bases generally produced only trace amounts of the desired macrocyclic products together with large amounts of intractable oligomers. This metal ion size-dependency suggests that the larger ions Cs<sup>+</sup> and K<sup>+</sup> may form more stable, tridentate chelates with tetrazole **1** than the smaller ions. We then designed tetrazole **9** (Table 1), suspecting that amido-H may form an internal hydrogen bond with tetrazole-N1 which should reinforce the bent nitrile imine geometry. Thus, tetrazole **9** was readily prepared through amidation of tetrazole **7** with 4-chloro-butanoyl chloride followed by an intramolecular *O*-alkylation. Notably, Na<sub>2</sub>CO<sub>3</sub> was found to be the optimal base for the ring closure reaction (compare entries 21–24).

The structures of macrocyclic tetrazoles **6** and **9** were confirmed by X-ray crystallography (Figure 1). To our surprise, the amide bond in **9** was engaged in a pair of intermolecular H-bonds between N5-H and N1 of the neighboring tetrazole instead of an internal one. The three conjoining aromatic rings are slightly twisted out of the tetrazole plane with the torsional angles of N1-N2-C2-C3 and N1-C1-C8-C13 to be 45.12° and -44.38°, respectively (for tetrazole **6**), and -62.46° and 37.17°, respectively (for tetrazole **9**). These distortions might be due to lone-pair repulsion between N1 and O1 (distance: 2.815 Å for **6**, 2.848 Å for **9**) and between N1 and O2 (distance: 2.857 Å for **6**, 3.249 Å for **9**).

To assess the reactivity of macrocyclic tetrazoles, we carried out the photoinduced cycloaddition reactions with either 4-penten-1-ol, an analogue of a bioorthogonal alkene reporter homoallylglycine,[15] or a strained alkene reporter norbornene[16] in ethyl acetate (Table 2). Because the reaction proceeds through two distinct steps: ring opening step to generate the cyclic nitrile imine in situ and the subsequent [3+2] cycloaddition reaction,[10] we monitored the reactions by thin layer chromatography and discontinued the reactions once the tetrazole starting materials were consumed. We found that in general macrocyclic tetrazoles gave higher yields of the pyrazoline cycloadducts (with exceptions of entries 5, 6, 11) compared to their acyclic counterparts (entries 7, 14). As expected, norbornene serves as a more reactive dipolarophile as compared with 4-penten-1-ol, affording the corresponding pyrazolines in higher yields (compare entries 8–14 to 1–7). Among the macrocyclic tetrazoles, the 3- and 4-carbon linked tetrazoles **2** and **3** showed markedly higher reactivity with shorter reaction times and higher yields (entries 2, 8, 9), presumably due to their smaller ring sizes and thus reduced conformational flexibility. It is interesting to note that *O*-xylylene-linked tetrazole **6** gave a moderate yield with 4-penten-1-ol (entry 5) but a good yield with norbornene (entry 12), which can be attributed to a compact exo TS stabilized by attractive edge-to-face C—H•••π interaction between norbornene bridge C—H and xylyl-π crowd.[17] Gratifyingly, the X-ray structure of pyrazoline **3b** was obtained, showing that the two phenyl rings are mostly co-planar with the pyrazoline ring with the torsional angles of N1-N2-C15-C16 and N1-C1-C9-C14 to be 30.8° and -26.6°, respectively (Figure 2).

The excellent reactivity of the macrocyclic tetrazoles toward norbornene prompted us to measure the photophysical properties of the resulting macrocyclic pyrazolines (Table 3). Relative to the pyrazoline control **10b** (entry 7), four macrocyclic pyrazolines showed the bathochromic shifts in λ<sub>abs</sub> (entries 1–2, 5–6) while two pyrazolines showed the

hypsochromic shifts (entries 3–4), presumably due to their twisted macrocyclic geometries. Compared to **10b**, macrocyclic pyrazolines exhibited invariable hypsochromic shifts in the maximum emission wavelength ( $\lambda_{em}$ ) along with increases in the fluorescence quantum yield ( $\phi_F$ ).

To examine whether the macrocyclic tetrazoles can be used to label a norbornene-containing protein, we incubated tetrazoles **2–6** (200  $\mu$ M) with a norbornene-modified lysozyme (10  $\mu$ M) in PBS buffer. The mixtures were photoirradiated with a handheld 302-nm UV lamp for 1 min prior to quenching with SDS sample buffer. In-gel fluorescence analysis (Figure 3) indicated that tetrazoles **2**, **3** and **6**, along with acyclic tetrazole **10**, showed specific pyrazoline cycloadducts, in good agreement with their generally higher reactivity (entries 8, 9 and 12 in Table 2) and their superior photophysical properties (entries 1, 2 and 5 in Table 3). In particular, tetrazole **6** showed the strongest fluorescent band, presumably due to rate enhancement in water as a result of tighter hydrophobic packing in the TS. However, initial efforts to determine the reaction yields using mass spectrometry were unsuccessful due to the poor solubility of the pyrazoline-cycloadducts in PBS buffer.

In summary, we have synthesized a series of structurally novel macrocyclic diphenyl tetrazoles by installing a short “bridge” between the two flanking diphenyl rings. Compared to the acyclic tetrazole, several macrocyclic tetrazoles showed improved reactivity toward a strained alkene both in organic solvent. One macrocyclic tetrazole showed rapid (~ 1 min) functionalization of a norbornene-modified protein in PBS buffer. These macrocyclic tetrazoles should offer a new class of photoactivatable tetrazole reagents for the bioorthogonal tetrazole-alkene cycloaddition reaction in living systems.

## Experimental Section

**Photoinduced Cycloaddition of Lyso-Norbornene with Macrocyclic Tetrazoles:** To a 20- $\mu$ L solution of either Lyso or Lyso-Nor (10  $\mu$ M) in PBS buffer, pH 7.4, in a 96-well microtiter plate was added 1  $\mu$ L of the various tetrazoles (4 mM in DMSO, final concentration is 200  $\mu$ M). The mixtures were irradiated with a handheld 302-nm UV lamp for 1 min before quenching by addition of 5  $\mu$ L of 6 $\times$  SDS sample buffer, boiled for 5 min at 95  $^{\circ}$ C, loaded onto a NuPAGE 12% Bis-Tris gel (Invitrogen), and then subjected to protein electrophoresis. The Lyso-Pyr cycloadducts in the gel were visualized by illuminating the gel with a handheld 365-nm UV lamp and the resulting image was captured by a digital camera. After the image acquisition, the same gel was stained with Coomassie blue to confirm the size and equal loading of proteins.

## Supplementary Material

Refer to Web version on PubMed Central for supplementary material.

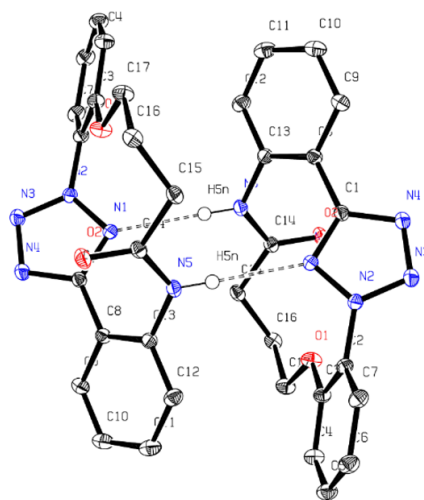
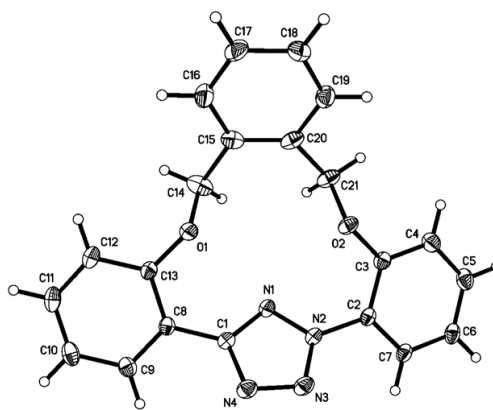
## Acknowledgments

We gratefully acknowledge the National Institutes of Health (GM 85092) for financial support. We thank William Brennessel at University of Rochester for X-ray structural determination. The crystal structures of **6**, **9**, and **3b** have been deposited into the Cambridge Crystallographic Data Centre with the deposit numbers of CCDC 783273, 783275 and 783274, respectively..

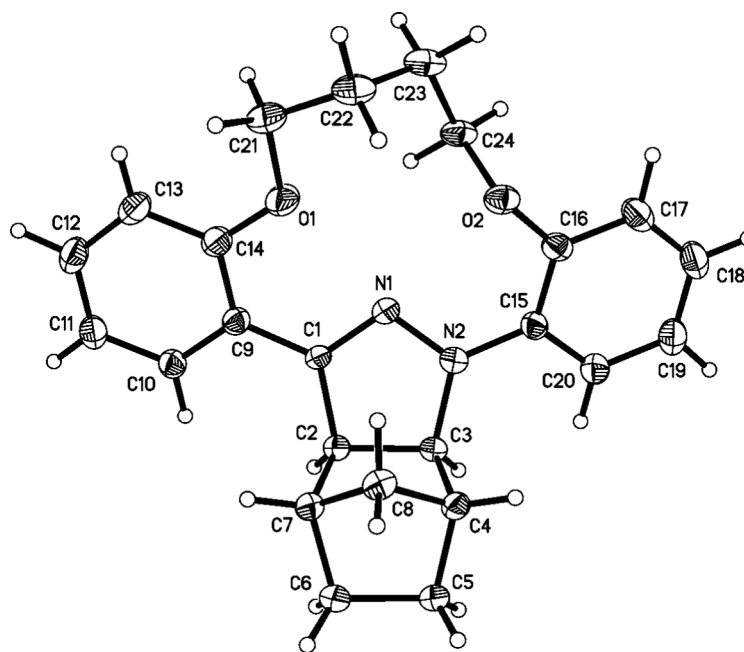
## References

1. a) Sletten EM, Bertozzi CR. *Angew Chem Int Ed.* 2009; 48:6974–6998. b) Lim RKV, Lin Q. *Chem Comm.* 2010; 46:1489–1600. c) Jewett JC, Bertozzi CR. *Chem Soc Rev.* 2010; 39:1272–1279. [PubMed: 20349533]

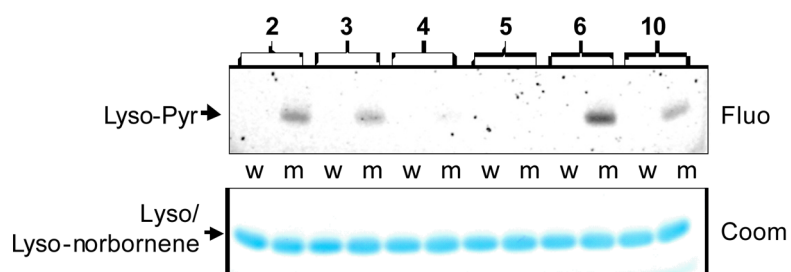
2. a) Rostovtsev VV, Green LG, Fokin VV, Sharpless KB. *Angew Chem Int Ed.* 2002; 41:2596–2599.  
b) Torne CW, Christensen C, Meldal M. *J Org Chem.* 2002; 67:3057–3064. [PubMed: 11975567]
3. For an excellent review, see: a) Debets MF, van der Doelen CW, Rutjes FP, van Delft FL. *ChemBiochem.* 2010; 11:1168–1184. [PubMed: 20455238] b) Agard NJ, Prescher JA, Bertozzi CR. *J Am Chem Soc.* 2004; 126:15046–15047. [PubMed: 15547999] c) Agard NJ, Baskin JB, Prescher JA, Lo A, Bertozzi CR. *ACS Chem Biol.* 2006; 1:644–648. [PubMed: 17175580] d) Baskin JM, Prescher JA, Laughlin ST, Agard NJ, Chang PV, Miller IA, Lo A, Codelli JA, Bertozzi CR. *Proc Natl Acad Sci USA.* 2007; 104:16793–16797. [PubMed: 17942682] e) Ning X, Guo J, Wolfert MA, Boons GJ. *Angew Chem Int Ed.* 2008; 47:2253–2255. f) Debets MF, van Berkel SS, Schoffelen S, Rutjes FP, van Hest JC, van Delft FL. *Chem Comm.* 2010; 46:97–99. [PubMed: 20024305] g) Jewett JC, Sletten EM, Bertozzi CR. *J Am Chem Soc.* 2010; 132:3688–3690. [PubMed: 20187640]
4. McKay CS, Moran J, Pezacki JP. *Chem Comm.* 2010; 46:931–933. [PubMed: 20107654]
5. a) Dorn H, Otto A. *Angew Chem Int Ed.* 1968; 7:214–215. b) Truce WE, Allison JR. *J Org Chem.* 1975; 40:2260–2261. c) Hashimoto T, Maeda Y, Omote M, Nakatsu H, Maruoka K. *J Am Chem Soc.* 2010; 132:4076–4077. [PubMed: 20199072]
6. a) Padwa A, Carter SP, Nimmegern H. *J Org Chem.* 1986; 51:1157–1158. b) Padwa A, Carter SP, Nimmegern H, Stull PD. *J Am Chem Soc.* 1988; 110:2894–2900. c) Padwa A, Fryxell GE, Zhi L. *J Am Chem Soc.* 1990; 112:3100–3109.
7. a) Pandey G, Bagul TD, Sahoo AK. *J Org Chem.* 1998; 63:760–768. [PubMed: 11672071] b) Pearson WH, Stoy P, Mi Y. *J Org Chem.* 2004; 69:1919–1939. [PubMed: 15058937] c) Coldham I, Burrell AJM, White LE, Adams H, Oram N. *Angew Chem Int Ed.* 2007; 46:6159–6162. d) Coldham I, Jana S, Watson L, Pilgram CD. *Tetrahedron Lett.* 2008; 49:5408–5410.
8. For a recent review, see: a) Revuelta J, Cicchi S, Goti A, Brandi A. *Synthesis.* 2007:485–504. b) Cardona F, Valenza S, Picasso S, Goti A, Brandi A. *J Org Chem.* 1998; 63:7311–7318. [PubMed: 11672377] c) Thiverny M, Philouze C, Chavant PY, Blandin V. *Org Biomol Chem.* 2010; 8:864–872. [PubMed: 20135045] d) Ghini G, Luconi L, Rossin A, Bianchini C, Giambastiani G, Cicchi S, Lascialfari L, Brandi A, Giannasi A. *Chem Comm.* 2010; 46:252–254. [PubMed: 20024342]
9. a) Huisgen R. *Angew Chem Int Ed.* 1963; 2:565–598. b) Huisgen R. *Angew Chem Int Ed.* 1963; 2:633–645. c) Bianchi, G.; Gandolfi, R. *1,3-Dipolar Cycloaddition Chemistry.* Padwa, A., editor. Wiley; New York: 1984. p. 470–477.
10. a) Wang Y, Vera CR, Lin Q. *Org Lett.* 2007; 9:4155–4158. [PubMed: 17867694] b) Song W, Wang Y, Qu J, Madden MM, Lin Q. *Angew Chem Int Ed.* 2008; 47:2832–2835. c) Wang Y, Hu WJ, Song W, Lim RKV, Lin Q. *Org Lett.* 2008; 10:3725–3728. [PubMed: 18671406] d) Song W, Yu Z, Madden MM, Lin Q. *Mol Biosys.* 2010; 6:1576–1578.
11. a) Song W, Wang Y, Qu J, Lin Q. *J Am Chem Soc.* 2008; 130:9654–9655. [PubMed: 18593155] b) Wang Y, Song W, Hu WJ, Lin Q. *Angew Chem Int Ed.* 2009; 48:5330–5333.
12. Zheng SL, Wang Y, Yu Z, Lin Q, Coppens P. *J Am Chem Soc.* 2009; 131:18036–18037. [PubMed: 19928921]
13. a) Ess DH, Houk KN. *J Am Chem Soc.* 2007; 129:10646–10647. [PubMed: 17685614] b) Ess DH, Houk KN. *J Am Chem Soc.* 2008; 130:10187–10198. [PubMed: 18613669] c) Schoenebeck F, Ess DH, Jones GO, Houk KN. *J Am Chem Soc.* 2009; 131:8121–8133. [PubMed: 19459632]
14. Ito S, Tanaka Y, Kakehi A, Kondo K. *Bull Chem Soc Jpn.* 1976; 49:1920–1923.
15. Song W, Wang Y, Yu Z, Rivera Vera CI, Qu J, Lin Q. *ACS Chem Biol.* 2010; 510.1021/cb100193h
16. a) Devaraj NK, Weissleder R, Hilderbrand SA. *Bioconjugate Chem.* 2008; 19:2297–2299. b) Gutmiedl K, Wirges CT, Ehmke V, Carell T. *Org Lett.* 2009; 11:2405–2408. [PubMed: 19405510] c) Han HS, Devaraj NK, Lee J, Hilderbrand SA, Weissleder R, Bawendi MG. *J Am Chem Soc.* 2010; 132:7838–7839. [PubMed: 20481508]
17. Paliwal S, Geib S, Wilcox CS. *J Am Chem Soc.* 1994; 116:4497–4498.



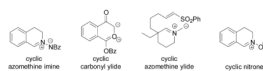
**Figure 1.** ORTEP diagrams of macrocyclic tetrazole **6** (top) and the dimer of macrocyclic tetrazole **9** (bottom) shown at 50% probability.



**Figure 2.**  
ORTEP diagram of the macrocyclic pyrazoline **3b** shown at 50% probability.



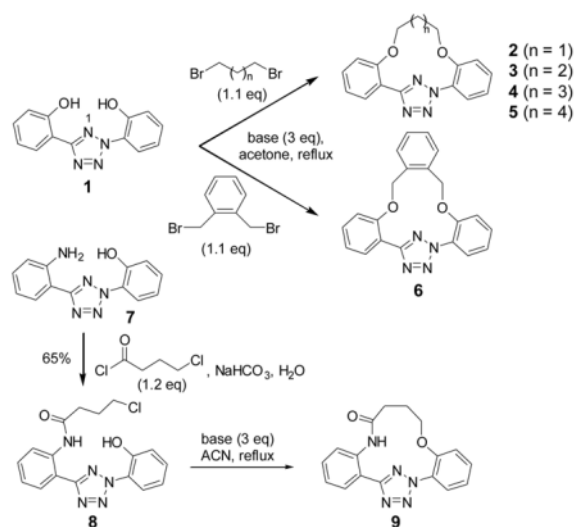
**Figure 3.** Photoinduced cycloaddition reaction of tetrazoles with a norbornene-modified lysozyme (m) or wild-type lysozyme (w) at 302 nm: top panel, inverted in-gel fluorescence with  $\lambda_{\text{ex}} = 365$  nm; bottom panel, Coomassie blue staining.



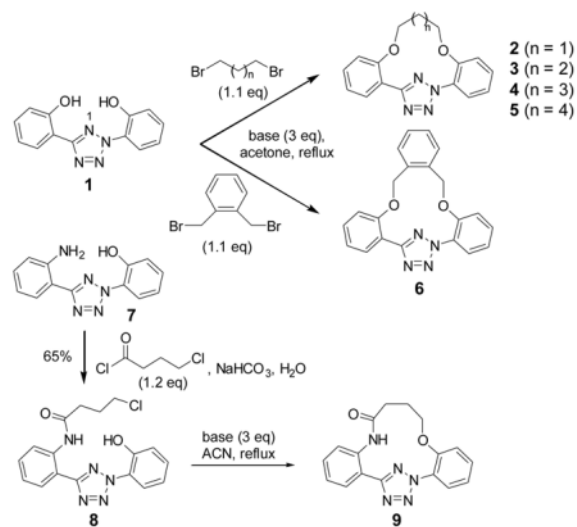
**Scheme 1.**  
Representative cyclic 1,3-dipoles.



Table 1

Synthesis of the macrocyclic tetrazoles<sup>[a]</sup>.

entry	base	product	yield (%) <sup>[b]</sup>
1	LiOH•H <sub>2</sub> O		trace
2	Na <sub>2</sub> CO <sub>3</sub>		<5 <sup>[c]</sup>
3	K <sub>2</sub> CO <sub>3</sub>		<30 <sup>[c]</sup>
4	Cs <sub>2</sub> CO <sub>3</sub>		38
5	LiOH•H <sub>2</sub> O		trace
6	Na <sub>2</sub> CO <sub>3</sub>		trace
7	K <sub>2</sub> CO <sub>3</sub>		51
8	Cs <sub>2</sub> CO <sub>3</sub>		78
9	LiOH•H <sub>2</sub> O		trace
10	Na <sub>2</sub> CO <sub>3</sub>		trace
11	K <sub>2</sub> CO <sub>3</sub>		<35 <sup>[c]</sup>
12	Cs <sub>2</sub> CO <sub>3</sub>		45
13	LiOH•H <sub>2</sub> O		trace
14	Na <sub>2</sub> CO <sub>3</sub>		trace
15	K <sub>2</sub> CO <sub>3</sub>		<60 <sup>[c]</sup>
16	Cs <sub>2</sub> CO <sub>3</sub>		67



entry	base	product	yield (%) <sup>[b]</sup>
17	LiOH•H <sub>2</sub> O		trace
18	Na <sub>2</sub> CO <sub>3</sub>		trace
19	K <sub>2</sub> CO <sub>3</sub>		<50 <sup>[c]</sup>
20	Cs <sub>2</sub> CO <sub>3</sub>	 <b>6</b>	61
21	LiOH•H <sub>2</sub> O		trace
22	Na <sub>2</sub> CO <sub>3</sub>	 <b>9</b>	70
23	K <sub>2</sub> CO <sub>3</sub>		<20 <sup>[c]</sup>
24	Cs <sub>2</sub> CO <sub>3</sub>		trace

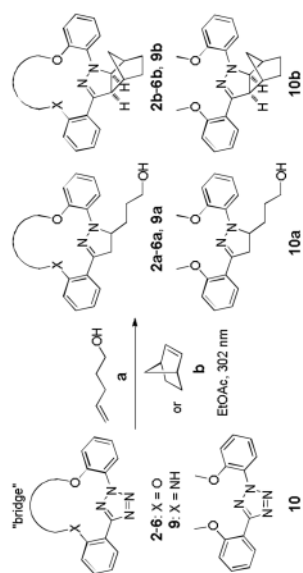
<sup>[a]</sup> For bis-O-alkylation, reactions were carried out by refluxing tetrazole **1** with 1.1 equiv of dibromide and 3 equiv of base in acetone overnight. For intramolecular O-alkylation, tetrazole **8** was refluxed in acetonitrile with 3 equiv of base.

<sup>[b]</sup> Isolated yields were reported unless noted otherwise.

<sup>[c]</sup> Estimated yields based on TLC.

Table 2

Photoinduced 1,3-Dipolar Cycloaddition Reactions of Macrocyclic and Acyclic Tetrazoles with Alkenes<sup>[a]</sup>.



entry	alkene	tetrazole	pyrazoline	time <sup>[b]</sup> (min)	yield <sup>[c]</sup> (%)
1		2	2a	120	59
2		3	3a	75	71
3		4	4a	84	60
4		5	5a	180	70
5		6	6a	120	46 <sup>[d]</sup>
6		9	9a	300	43
7		10	10a	120	58
8		2	2b	108	95
9		3	3b	54	91
10		4	4b	120	81
11		5	5b	240	60
12		6	6b	90	84
13		9	9b	120	84
14		10	10b	60	76

<sup>[a]</sup> Reactions were conducted by irradiating 0.1 mmol of tetrazole and 10 mmol of alkene dipolarophile in 250 mL EtOAc with a 302-nm UV lamp in quartz flask.

<sup>[b]</sup> Time was determined by tracing the disappearance of the starting materials on TLC.

<sup>[c]</sup> Isolated yields.

<sup>[d]</sup> The pyrazoline adduct was unstable upon standing.

Table 3

Photophysical properties of macrocyclic pyrazolines<sup>[a]</sup>.

entry	pyrazoline	$\lambda_{\text{abs}}$ (nm)	$\epsilon$ ( $\text{M}^{-1} \text{cm}^{-1}$ )	$\lambda_{\text{em}}$ (nm) <sup>[b]</sup>	$\phi_{\text{f}}$ <sup>[c]</sup>
1	<b>2b</b>	358	20,356	456	0.30
2	<b>3b</b>	364	10,190	466	0.35
3	<b>4b</b> <sup>[d]</sup>	348	1,702	468	0.35
4	<b>5b</b> <sup>[d]</sup>	348	830	464	0.17
5	<b>6b</b>	358	13,852	451	0.32
6	<b>9b</b>	376	19,440	477	0.25
7	<b>10b</b>	350	12,534	502	0.15

<sup>[a]</sup> Compounds were dissolved in PBS:ACN (1:1) at the concentrations of 5  $\mu\text{M}$  unless noted otherwise.<sup>[b]</sup>  $\lambda_{\text{ex}}$  = 348 nm.<sup>[c]</sup> Quantum yields were determined using DAPI as the standard ( $\phi_{\text{f}}$  = 0.58 in DMSO).<sup>[d]</sup> 20  $\mu\text{M}$  concentrations were used.